Lawrence Berkeley National Laboratory

Title

Multiple topological Dirac cones in a mixed-valent Kondo semimetal: g-SmS

Permalink

Journal

ISSN

Authors

Kang, Chang-Jong
Ryu, Dong-Choon
Kim, Junwon
et al.

Publication Date

DOI

Peer reviewed

Multiple topological Dirac cones in a mixed-valent Kondo semimetal: g-SmS

Chang-Jong Kang[1],[*] Dong-Choon Ryu[2],[*] Junwon Kim[2], Kyoo Kim[2],[3], J.-S. Kang[4], J. D. Denlinger[5], G. Kotliar[1],[6], and B. I. Min[2][†]

[1]*Department of Physics and Astronomy, Rutgers University, Piscataway, New Jersey 08854, USA*
[2]*Department of Physics, Pohang University of Science and Technology, Pohang 37673, Korea*
[3]*MPPHC_CPM, Pohang University of Science and Technology, Pohang 37673, Korea*
[4]*Department of Physics, The Catholic University of Korea, Bucheon 14662, Korea*
[5]*Advanced Light Source, Lawrence Berkeley Laboratory, Berkeley, California 94720, USA*
[6]*Condensed Matter Physics and Materials Science Department,*
Brookhaven National Laboratory, Upton, New York 11973, USA
(Dated: August 16, 2019)

We demonstrate theoretically that the golden phase of SmS (g-SmS), a correlated mixed-valent system, exhibits nontrivial surface states with diverse topology. It turns out that this material is an ideal playground to investigate different band topologies in different surface terminations. We have explored surface states on three different (001), (111), and (110) surface terminations. Topological signature in the (001) surface is not apparent due to a hidden Dirac cone inside the bulk-projected bands. In contrast, the (111) surface shows a clear gapless Dirac cone in the gap region, demonstrating the unambiguous topological Kondo nature of g-SmS. Most interestingly, the (110) surface exhibits both topological-insulator-type and topological-crystalline-insulator (TCI)-type surface states simultaneously. Two different types of double Dirac cones, Rashba-type and TCI-type, realized on the (001) and (110) surfaces, respectively, are analyzed with the mirror eigenvalues and mirror Chern numbers obtained from the model-independent *ab initio* band calculations.

PACS numbers:

Introduction. Topological insulators have been studied intensively in recent years as a new phase of quantum matter and for possible applications to spintronics and quantum computing [1, 2]. The physical significance of topological insulators is that they possess metallic surface states that are protected by time-reversal symmetry, which leads to the exhibition of robust surface states under any perturbations without breaking the symmetry [1, 2]. Since the theoretical study proposed that nontrivial topology emerges in strongly correlated mixed-valent or Kondo systems [3, 4], subsequent experiments have been conducted to examine the topological properties in a candidate material SmB_6 [5–18]. Several angle-resolved photoemission spectroscopy (ARPES) measurements confirmed a topologically-driven metallic surface state [11–15] and its spin helicity in the (001) surface [16], where these topological properties are induced solely from a single Dirac cone. But a few ARPES reports claim that the observed surface states are just trivial [17, 18]. So the controversy still remains.

Another candidate for a topological Kondo material was proposed theoretically in a Sm mixed-valent/Kondo system, golden phase of SmS (g-SmS). But, unlike SmB_6 that has a simple-cubic structure, g-SmS crystallizes in rock-salt-type face-centered cubic (fcc) structure and has a semi-metallic electronic structure. The difference in crystal symmetry gives rise to a richer or more intricate topological structure. Due to the odd number of band inversions in the bulk band structure, g-SmS was suggested to be a topological compensated semimetal [19]. However, (001) surface states exhibit double Dirac cones

with a tiny gap instead of gapless Dirac cones [20]. This result is in contrast with that of Kasinathan *et al.* [21], who reported the existence of gapless Dirac cones on the (001) surface of the isoelectronic compound SmO. Thus whether a gap exists in the double Dirac cones on the (001) surface of g-SmS is still unclear, which is an important issue to be clarified in connection with its topological nature.

The double Dirac cones appear when two single-Dirac cones, which are induced from band inversion at non-
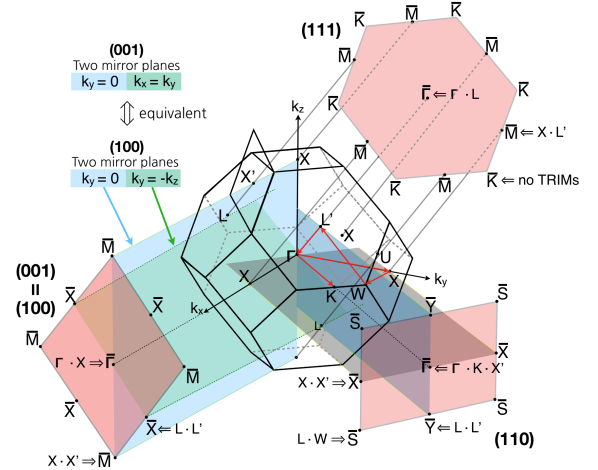
FIG. 1: (Color Online) Bulk and surface BZs of fcc g-SmS. There are mirror-symmetry lines along $\bar{\Gamma} - \bar{M}$ and $\bar{\Gamma} - \bar{X}$ on the (100) surface BZ, and along $\bar{\Gamma} - \bar{X}$ and $\bar{\Gamma} - \bar{Y}$ on the (110) surface BZ.
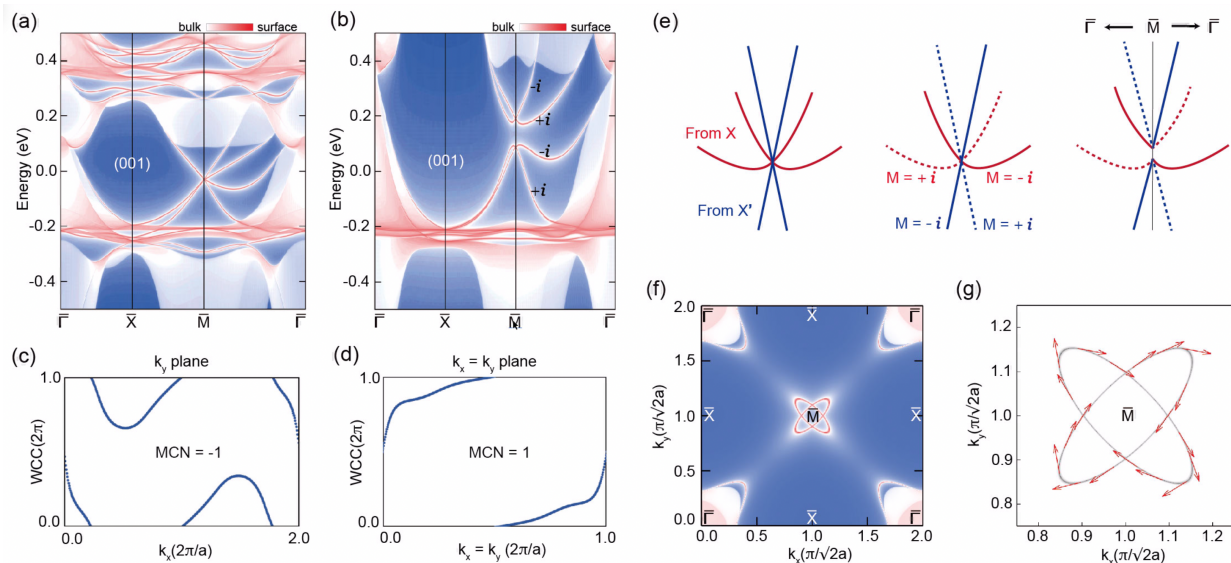
FIG. 2: (Color Online) Semi-infinite TB slab calculations for the (001) surface of g-SmS with (a) normal SOC and (b) the enhanced SOC strength by ten times. While the gap in the double Dirac cones in (a) is too tiny to be identified, the gap is clearly shown in (b) with the enhanced SOC strength. Mirror eigenvalues along $\bar{\Gamma}-\bar{M}$ are denoted in (b). (c),(d) The evolutions of the Wannier charge centers (WCCs), respectively, for $k_y = 0$ and $k_x = k_y$ mirror-symmetry planes. Two distinct MCNs, $(C_0, C_d) = (-1, +1)$, are obtained from the Wilson-loop calculations. (e) Schematic diagram for the gap-opening mechanism in the double Dirac cones along $\bar{\Gamma}-\bar{M}-\bar{\Gamma}$ (see Fig. 1). The bands having the same mirror eigenvalue (M) hybridize with each other to produce the energy gap. (f),(g) The FS, and its spin texture around $\bar{M}$. The spin texture shows the Rashba-type spin polarization. For the comparison to experiment, one needs to take into account the scale factor of $Z \approx 0.1$ in the y-axis DFT energies in (a) and (b) due to the band renormalization effect.

equivalent bulk k-points, are projected onto one k-point in the surface Brillouin zone (BZ) (see Fig. 1). The double Dirac cones were detected in ARPES measurements for CeBi [22, 23] and also for topological-crystalline insulators (TCIs) [24] of SnTe [25–27] and SnSe [28, 29], having the same rock-salt structure as g-SmS. Note that double Dirac cones observed in the Sn-chalcogenides have basically different topology from those in CeBi. The Sn-chalcogenides have the gapless double Dirac cones, while CeBi has the gapped double Dirac cones. Therefore, it is imperative to identify the topological nature of the double Dirac cones realized in g-SmS.

In this work, we have investigated the surface states of g-SmS, which is one of the representative Sm compounds exhibiting mixed-valent Kondo properties, employing the density functional theory (DFT) and the Wilson-loop calculations. The strong correlation effect of $4f$ electrons in Kondo systems can be captured by renormalizing DFT $4f$ bands with a reasonable scale factor. Indeed we have shown before that the DFT band structures near the Fermi level (E_F) have similar shape to those obtained by the dynamical mean-field theory (DMFT) at low temperature after rescaling the DFT band with the DMFT renormalization factors [14, 20, 30, 31]. With this rescaling in the bulk, the slab calculations properly describe the surface states [32].

Here we have demonstrated for g-SmS that (i) it has

nontrivial mirror Chern numbers (MCNs), (ii) the (001) surface has the gapped double Dirac cones seemingly of Rashba-type, (iii) the (111) surface has a clear single Dirac cone in the gap region, confirming that g-SmS is indeed a topological Kondo system, and (iv) the (110) surface has the TCI-type double Dirac cones as well as the intriguing topological-insulator (TI)-type single Dirac cone.

Method. For the DFT calculations, we have used the projector-augmented wave band method [33], implemented in VASP [34]. We have employed the generalized-gradient approximation [35] for the exchange-correlation functional. A lattice constant of $a = 5.6$ $\mathring{A}$ was used for g-SmS. To investigate surface electronic structures, we have constructed the tight-binding (TB) Hamiltonian from DFT results, using the Wannier interpolation scheme implemented in WANNIER90 code [36], and then

TABLE I: Products of parity eigenvalues of the occupied states at the time-reversal invariant momentum (TRIM) points of the bulk BZ of fcc g-SmS. It indicates nontrivial Z_2 topology.

	Γ	$3\,X$	$4\,L$	Z_2
g-SmS	+	−	+	1

performed semi-infinite TB slab calculations using the Green function method [37] implemented in Wannier-Tools [38]. We have double-checked the surface band structures by performing the DFT slab calculations with both the WIEN2K [39] and the VASP [34] codes. The topological nature of surface states is analyzed in terms of the mirror eigenvalues and MCNs [40–44], which are obtained from the Wilson-loop calculations [45, 46] based on the model-independent *ab initio* calculations.

(001) surface. Since *g*-SmS shows Sm 4*f*-5*d* band inversion at X of the bulk BZ [19, 20], it provides a nontrivial Z_2 number, as shown in Table I. On the (001) surface of *g*-SmS, one X point is projected onto $\bar{\Gamma}$, while two non-equivalent bulk X points (X and X' in Fig. 1) are projected onto the $\bar{M}$ point of the surface BZ, and so the single and double Dirac cones are expected to be realized, respectively, at $\bar{\Gamma}$ and $\bar{M}$.

Figure 2 shows the (001) surface band structures obtained from semi-infinite TB slab calculations. The single Dirac cone at $\bar{\Gamma}$ is hardly detectable in Fig. 2(a) due to an overlap with the bulk band structures. On the other hand, the double Dirac cones are noticeable at $\bar{M}$, which seem to be gapless as claimed by Kasinathan *et al.* [21] for SmO. However, a tiny band gap actually exists. The gap opening is clearly identified for the calculation with ten-times enhanced spin-orbit coupling (SOC) strength in Fig. 2(b) [47], which manifests the gapped double Dirac cones of Rashba-type in agreement with a previous report [20]. As shown in Fig. 1, on the (001) surface, there are two mirror-symmetry lines along $\bar{\Gamma} - \bar{X}$ and $\bar{\Gamma} - \bar{M}$. Therefore, the gap opening along $\bar{X} - \bar{M}$ is obvious because there is no mirror symmetry to protect the band crossings. But, further analysis is required for the surface states along $\bar{\Gamma} - \bar{M}$.

To explore the origin of the gap opening along $\bar{\Gamma} - \bar{M}$, we have calculated MCNs and the mirror eigenvalues of the surface states. In the bulk BZ, there are two independent mirror-symmetry planes: the $k_y = 0$ and $k_x = k_y$ planes [48]. Note that two mirror operators with respect to the $k_y = 0$ and $k_y = \pi$ planes are symmetrically equivalent. Therefore *g*-SmS has two independent MCNs, $C_0(\equiv C_{k_y=0}^+)$ and $C_d(\equiv C_{k_x=k_y}^+)$, where the '+' sign refers to the mirror eigenvalue of $+i$ for the corresponding mirror-symmetry plane.

Figures 2(c) and 2(d) show the evolutions of the Wannier charge centers (WCCs) for the $k_y = 0$ and $k_x = k_y$ mirror planes. The corresponding MCNs are obtained to be $C_0 = -1$ and $C_d = 1$, which implies the existence of at least one gapless Dirac cone along both $\bar{M} - \bar{\Gamma} - \bar{M}$ and $\bar{X} - \bar{\Gamma} - \bar{X}$ lines on the (001) surface (see Fig. 1). Accordingly, the MCN of $C_0 = -1$ is suggestive of ruling out the existence of additional gapless Dirac cones along $\bar{\Gamma} - \bar{M}$ besides the gapless single Dirac cone buried at $\bar{\Gamma}$. Indeed, mirror eigenvalue analysis provides a more direct explanation on the gapping. Depicted schematically in Fig. 2(e) are the double Dirac cones along $\bar{\Gamma} - \bar{M} - \bar{\Gamma}$,
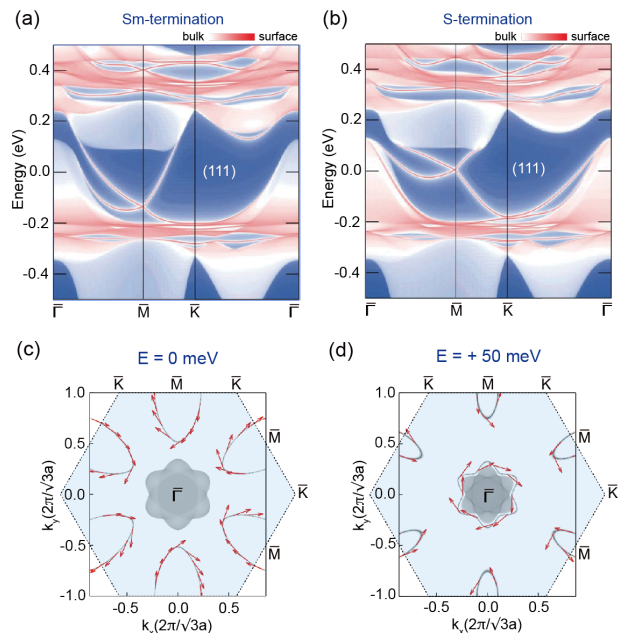

FIG. 3: (Color Online) Surface electronic structures from the semi-infinite TB slab calculations for the (111) surface of *g*-SmS with (a) Sm- and (b) S-termination. Topological Dirac-cone surface states are clearly shown at $\bar{M}$ in both (a) and (b). (c),(d) The FS and the energy contour at $E = 50$ meV, respectively, for the Sm-terminated case. Their spin textures with spin helicities of Rashba-type are also provided.

which are composed of two single Dirac cones arising from band inversions at two non-equivalent bulk X points, X (red) and X' (blue). Two bands of each single Dirac cone have opposite mirror eigenvalues: $+i$ for the dotted and $-i$ for the solid line in Fig. 2(e). Then the crossing Dirac-cone bands with the same mirror eigenvalues hybridize with each other to produce the hybridization gap around $\bar{M}$, resulting in the gapped double Dirac cones. Namely, the double Dirac cones at $\bar{M}$ have neither the TI nor the TCI character [24]. As mentioned earlier, this kind of double Dirac-cone feature around $\bar{M}$ was detected in ARPES for CeBi [22, 23]. Note, however, that the double Dirac cones detected in CeBi appear due to a *p-d* (not *f-d*) band inversion.

Figure 2(f) presents the Fermi surface (FS) of the (001) surface band structure with normal SOC strength. The crossing oval-shaped FS is apparent around $\bar{M}$, which arises from the double Dirac cones at $\bar{M}$ in Fig. 2(a). On the other hand, the FS around $\bar{\Gamma}$ is derived from both bulk and surface band structures. The spin texture of the FS around $\bar{M}$ is provided in Fig. 2(g). The spin-helical structure around each ellipse is evident, reflecting that the gapped double Dirac cones have the spin texture of Rashba-type (not Dresselhaus-type) [41–44].

(111) surface. In order to ascertain the topological nature of *g*-SmS more evidently, we have investigated the (111) surface states. As shown in Fig. 1, each non-
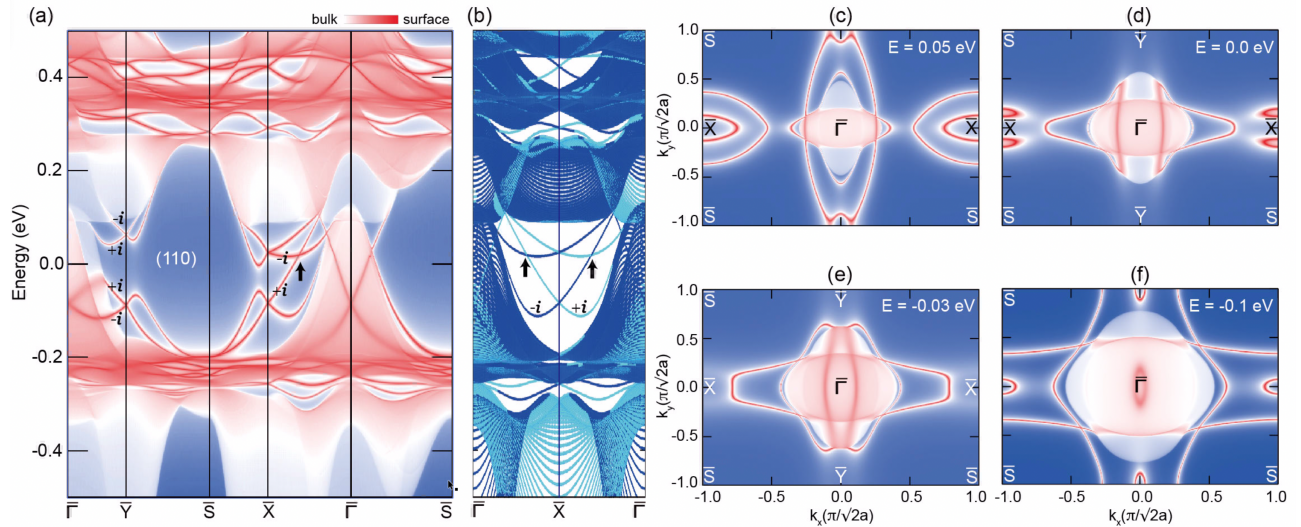
FIG. 4: (Color Online) (a) Semi-infinite TB slab calculations for the (110) surface of g-SmS. The double Dirac cones of TCI-type are clearly manifested around $\bar{X}$. A single Dirac-cone surface state is also seen at $\bar{\Gamma}$, even though it is buried inside the bulk-projected bands. (b) Mirror eigenvalues of the double Dirac cones along $\bar{\Gamma} - \bar{X} - \bar{\Gamma}$. Mirror eigenvalues of $+i$ and $-i$ are presented in aqua and navy-blue colors, respectively. (c)-(f) The FS and energy contours on the (110) surface.

equivalent bulk X point is projected onto a different $\bar{M}$ point of surface BZ on the (111) surface. Hence, the gapless single Dirac cone could be realized at each $\bar{M}$ point. Note that the (111) surface has two kinds of terminations: Sm- and S-terminations. As shown in Figs. 3(a) and 3(b), both terminations indeed possess the gapless single Dirac cone at $\bar{M}$ in the gap region. Figures 3(c) and 3(d) show the FS and the energy contour at $E = 50$ meV, respectively, for the Sm-terminated case. They clearly reveal the helical spin textures of Rashba-type, which originate from the single Dirac-cone surface states. These features provide unambiguous evidence of the topological nature in semimetallic g-SmS.

(110) surface. As in the case of the (001) surface, two non-equivalent bulk X points (X and X') are projected onto $\bar{X}$ of the (110) surface BZ (see Fig. 1). So the (110) surface also has double Dirac cones at $\bar{X}$. It is thus worthwhile to check whether these double Dirac cones at $\bar{X}$ would produce the TCI-type or the Rashba-type surface states as in the (001) surface. As shown in Fig. 4(a), the double Dirac cones at $\bar{X}$ manifest a hallmark of TCI-type surface states with a Dirac point off the TRIM points (marked by an arrow). They are gapped along $\bar{S} - \bar{X}$ because $\bar{S} - \bar{X}$ is not a mirror-symmetry line, while, along the mirror-symmetry line $\bar{X} - \bar{\Gamma}$, they show the prominent Dirac point in the gap region. To ensure the band crossing in-between $\bar{X} - \bar{\Gamma}$, we have analyzed their mirror eigenvalues. It is shown in Fig. 4(b) that the crossing surface bands have opposite mirror eigenvalues, $+i$ and $-i$, so that the band crossings are protected by the mirror symmetry, which is distinct from the case of the (001) surface. Note that, besides the double Dirac cones at $\bar{X}$, the (110) surface exhibits a single Dirac cone

of TI-type at $\bar{\Gamma}$ in Fig. 4(a). Its Dirac point is clearly manifested at $\bar{\Gamma}$, even though it is buried inside the bulk-projected bands at $E \approx -0.1$ eV.

As shown in Fig. 4(c)-(f), the energy contours around $\bar{X}$ display the Lifshitz-like transition as a function of binding energies, which is another manifestation of the TCI-type double Dirac-cone surface states [25]. However, the energy contours around $\bar{\Gamma}$ look more complicated than a single Dirac cone. This intricate features are expected to come from the TI-type single Dirac-cone surface state distorted along the other mirror-symmetry line, $\bar{\Gamma} - \bar{Y}$. As shown in Fig. 4(a), two neighboring surface states along $\bar{\Gamma} - \bar{Y}$, one of which corresponds to the Dirac-cone state and the other to a trivial state, have the same mirror eigenvalues, $+i$, and so they are hybridized to be gapped. Hence, most interestingly, the (110) surface has both the TCI and the intricate TI nature. It is noteworthy that this kind of TI/TCI feature was also proposed in the (110) surface of SmB_6 [40–44]. But one should keep in mind that they have different crystal structures, fcc g-SmS vs simple-cubic SmB_6, which induce different mirror symmetries in the two materials.

Finally, we would like to comment on the experimental verification of the topological nature of g-SmS. Note that g-SmS is a phase under pressure [20]. Therefore, it is not easy to probe its topological fingerprints by employing conventional ARPES because it is difficult to apply external pressure in ARPES. Instead of applying external pressure, one may utilize chemical pressure or strain to simulate the g-SmS phase with a reduced volume. For example, Y-substituted SmS ($Sm_{1-x}Y_xS$) or SmS-film grown on an iso-structural sulphide having a smaller volume can be used. In fact, ARPES measurements have

been performed on metallic $Sm_{1-x}Y_xS$ [49, 50], but no surface state has been observed yet.

Conclusion. We have demonstrated that g-SmS has the gapless single Dirac cone in the gap region of its (111) surface BZ, which provides unambiguous evidence of the topological Kondo nature in mixed-valent g-SmS. The double Dirac cones realized in the (001) and (110) surfaces of g-SmS result in the Rashba-type and TCI-type surface states, respectively, which are elaborated by the mirror eigenvalues and MCNs, obtained by *ab initio* band structure calculations. It is thus worth challenging experimentalists to identify, via high-resolution ARPES, the gapped double Dirac cones of Rashba-type surface states, the gapless TI-type Dirac cone, and the TCI-type double Dirac cones, respectively, for the (001), (111), and (110) surfaces of g-SmS or $Sm_{1-x}Y_xS$.

---

* Co-first authors
† Corresponding author: bimin@postech.ac.kr

[1] M. Z. Hasan and C. L. Kane, Rev. Mod. Phys. **82**, 3045 (2010).
[2] X.-L. Qi and S.-C. Zhang, Rev. Mod. Phys. **83**, 1057 (2011).
[3] M. Dzero, K. Sun, V. Galitski, and P. Coleman, Phys. Rev. Lett. **104**, 106408 (2010).
[4] M. Dzero, K. Sun, P. Coleman, and V. Galitski, Phys. Rev. B **85**, 045130 (2012).
[5] S. Wolgast, Ç. Kurdak, K. Sun, J. W. Allen, D.-J. Kim, and Z. Fisk, Phys. Rev. B **88**, 180405(R) (2013).
[6] D. J. Kim, S. Thomas, T. Grant, J. Botimer, Z. Fisk, and J. Xia, Sci. Rep. 3, 3150 (2013).
[7] D. J. Kim, J. Xia, and Z. Fisk, Nat. Mater. **13**, 466 (2014).
[8] S. Rößer, T.-H. Jang, D.-J. Kim, L. H. Tjeng, Z. Fisk, F. Steglich, and S. Wirth, Proc. Natl. Acad. Sci. U.S.A. **111**, 4798 (2014).
[9] L. Jiao, S. Rößer, D. J. Kim, L. H. Tjeng, Z. Fisk, F. Steglich, and S. Wirth, Nat. Commun. **7**, 13762 (2016).
[10] G. Li, Z. Xiang, F. Yu, T. Asaba, B. Lawson, P. Cai, C. Tinsman, A. Berkley, S. Wolgast, Y. S. Eo, D.-J. Kim, C. Kurdak, J. W. Allen, K. Sun, X. H. Chen, Y. Y. Wangm Z. Fisk, and Lu Li, Science **346**, 1208 (2014).
[11] N. Xu, X. Shi, P. K. Biswas, C. E. Matt, R. S. Dhaka, Y. Huang, N. C. Plumb, M. Radović, J. H. Dil, E. Pom-

[12] jakushina, K. Conder, A. Amato, Z. Salman, D. McK. Paul, J. Mesot, H. Ding, and M. Shi, Phys. Rev. B **88**, 121102(R) (2013).
[12] J. Jiang, S. Li, T. Zhang, Z. Sun, F. Chen, Z. R. Ye, M. Xu, Q. Q. Ge, S. Y. Tan, X. H. Niu, M. Xia, B. P. Xie, Y. F. Li, X. H. Chen, H. H. Wen, and D. L. Feng, Nat. Commun. **4**, 3010 (2013).
[13] M. Neupane, N. Alidoust, S.-Y. Xu, T. Kondo, Y. Ishida, D. J. Kim, C. Liu, I. Belopolski, Y. J. Jo, T.-R. Chang, H.-T. Jeng, T. Durakiewicz, L. Balicas, H. Lin, A. Bansil, S. Shin, Z. Fisk, and M. Z. Hasan, Nat. Commun. 4, 2991 (2013).
[14] J. D. Denlinger, J. W. Allen, J.-S. Kang, K. Sun, J.-W. Kim, J. H. Shim, B. I. Min, D.-J. Kim, and Z. Fisk, arXiv:1312.6637 (2013).
[15] C.-H. Min, P. Lutz, S. Fiedler, B. Y. Kang, B. K. Cho, H.-D. Kim, H. Bentmann, and F. Reinert, Phys. Rev. Lett. **112**, 226402 (2014).
[16] N. Xu, P. K. Biswas, J. H. Dil, R. S. Dhaka, G. Landolt, S. Muff, C. E. Matt, X. Shi, N. C. Plimb, M. Radović, E. Pomjakushina, K. Conder, A. Amato, S. V. Borisenko, R. Yu, H.-M. Weng, Z. Fang, X. Dai, J. Mesot, H. Ding, and M. Shi, Nat. Commun. **5**, 4566 (2014).
[17] Z.-H. Zhu, A. Nicolaou, G. Levy, N. P. Butch, P. Syers, X. F. Wang, J. Paglione, G. A. Sawatzky, I. S. Elfimov, and A. Damascelli, Phys. Rev. Lett. **111**, 216402 (2013).
[18] P. Hlawenka, K. Siemensmeyer, E. Weschke, A. Varykhalov, J. Sánchez-Barriga, N. Y. Shitsevalova, A. V. Dukhnenko, V. B. Filipov, S. Gabáni, K. Flachbart, O. Rader, and E. D. L. Rienks, Nat. Commun. **9**, 517 (2018).
[19] Z. Li, J. Li, P. Blaha, and N. Kioussis, Phys. Rev. B **89**, 121117(R) (2014).
[20] C.-J. Kang, H. C. Choi, K. Kim, and B. I. Min, Phys. Rev. Lett. **114**, 166404 (2015).
[21] D. Kasinathan, K. Koepernik, L. H. Tjeng, and M. W. Haverkort, Phys. Rev. B **91**, 195127 (2015).
[22] K. Kuroda, M. Ochi, H. S. Suzuki, M. Hirayama, M. Nakayama, R. Noguchi, C. Bareille, S. Akebi, S. Kunisada, T. Muro, M. D. Watson, H. Kitazawa, Y. Haga, T. K. Kim, M. Hoesch, S. Shin, R. Arita, and T. Kondo, Phys. Rev. Lett. **120**, 086402 (2018).
[23] P. Li, Z. Wu, F. Wu, C. Cao, C. Guo, Y. Wu, Y. Liu, Z. Sun, C.-M. Cheng, D.-S. Lin, F. Steglich, H. Yuan, T.-C. Chiang, and Y. Liu, Phys. Rev. B **98**, 085103 (2018).
[24] L. Fu, Phys. Rev. Lett. **106**, 106802 (2011).
[25] T. H. Hsieh, H. Lin, J. Liu, W. Duan, A. Bansil, and L. Fu, Nat. Commun. **3**, 982 (2012).
[26] Y. Tanaka, Z. Ren, T. Sato, K. Nakayama, S. Souma, T. Takahashi, K. Segawa, and Y. Ando, Nat. Phys. **8**, 800 (2012).
[27] S.-Y. Xu, C. Liu, N. Alidoust, M. Neupane, D. Qian, I. Belopolski, J. D. Denlinger, Y. J. Wang, H. Lin, L. A. Wray, G. Landolt, B. Slomski, J. H. Dil, A. Marcinkova, E. Morosan, Q. Gibson, R. Sankar, F. C. Chou, R. J. Cava, A. Bansil, and M. Z. Hasan, Nat. Commun. **3**, 1192 (2012).
[28] P. Dziawa, B. J. Kowalski, K. Dybko, R. Buczko, A. Szczerbakow, M. Szot, E. Łusakowska, T. Balasubramanian, B. M. Wojek, M. H. Berntsen, O. Tjernberg, and T. Story, Nat. Mater. **11**, 1023 (2012).
[29] Y. Okada, M. Serbyn, H. Lin, D. Walkup, W. Zhou, C. Dhital, M. Neupane, S. Xu, Y. J. Wang, R. Sankar, F. Chou, A. Bansil, M. Z. Hasan, S. D. Wilson, L. Fu, and

V. Madhavan, Science **341**, 1496 (2013).

[30] J. Kim, K. Kim, C.-J. Kang, S. Kim, H. C. Choi, J.-S. Kang, J. D. Denlinger, and B. I. Min, Phys. Rev. B **90**, 075131 (2014).

[31] C.-J. Kang, J. Kim, K. Kim, J. Kang, J. D. Denlinger, and B. I. Min, J. Phys. Soc. Jpn. **84**, 024722 (2015).

[32] For g-SmS, a proper value of Z is known to be around 0.1 (see Ref. [20]).

[33] G. Kresse and D. Joubert, Phys. Rev. B **59**, 1758 (1999).

[34] G. Kresse and J. Furthmüller, Phys. Rev. B **54**, 11169 (1996); Comput. Mater. Sci. **6**, 15 (1996).

[35] J. P. Perdew, K. Burke, and M. Ernzerhof, Phys. Rev. Lett. **77**, 3865 (1996).

[36] A. A. Mostofi, J. R. Yates, G. Pizzi, Y. S. Lee, I. Souza, D. Vanderbilt, N. Marzari, Comput. Phys. Commun. **185**, 2309 (2014).

[37] M. P. Lopez Sancho, J. M. Lopez Sancho, and J. Rubio, J. Phys. F : Met. Phys. **15**, 851 (1985).

[38] Q. S. Wu, S. N. Zhang, H.-F. Song, M. Troyer, and A. A. Soluyanov, Comput. Phys. Commun. **224**, 405 (2018).

[39] P. Blaha, K. Schwarz, G. K. H. Madsen, D. Kvasnicka, and J. Luitz, WIEN2K (Karlheinz Schwarz, Technische Universitat Wien, Austria, 2001).

[40] M. Ye, J. W. Allen, and K. Sun, arXiv:1307.7191 (2013).

[41] M. Legner, A. Rüegg, and M. Sigrist, Phys. Rev. Lett.

[42] P. P. Baruselli and M. Vojta, Phys. Rev. Lett. **115**, 156405 (2015).

[43] P. P. Baruselli and M. Vojta, Phys. Rev. Lett. **115**, 156404 (2015).

[43] P. P. Baruselli and M. Vojta, Phys. Rev. B **93**, 195117 (2016).

[44] M. Legner, A. Rüegg, and M. Sigrist, Phys. Rev. B **89**, 085110 (2014).

[45] R. Yu, X. L. Qi, A. Bernevig, Z. Fang and X. Dai, Phys. Rev. B **84**, 075119 (2011).

[46] A. A. Soluyanov and D. Vanderbilt, Phys. Rev. B **83**, 235401 (2011).

[47] We used ten-times larger SOC in Fig. 2(b) to enhance the visibility of an existing tiny gap. It could, however, be a better representation of reality by shifting up the SOC-split $j = 7/2$ states so as to remove incorrect interaction with surface states near E_{F}.

[48] Here we conisdered the (001) surface instead of the (100) surface.

[49] K. Imura, T. Hajiri, M. Matsunami, S. Kimura, M. Kaneko, T. Ito, Y. Nishi, N. K. Sato, and H. S. Suzuki, J. Korean Phys. Soc. **62**, 2028 (2013).

[50] M. Kaneko, M. Saito, T. Ito, K. Imura, T. Hajiri, M. Matsunami, S. Kimura, H. S. Suzuki, N. K. Sato, JPS Conf. Proc. **3**, 011080 (2014).